

Electrochemical and Stress Corrosion Behaviors of 316L Stainless Steel in the Borate solution

Lan Jin¹, Yier Guo², Feng Liu^{3*},

¹ College of Pipeline and Civil Engineering, China University of Petroleum (East China), Qingdao 266580, China

² College of Mechanical Engineering and Applied Electronics Technology, Beijing University of Technology, Beijing 100124, China

³ School of Mechanical Engineering, Liaoning Shihua University, Fushun 113001, China

*E-mail: liuf20000@163.com

Received: 20 December 2019 / *Accepted:* 19 February 2020 / *Published:* 10 April 2020

The electrochemical characteristics and stress corrosion behavior of 316L stainless steel in the borate solution with different pH were investigated through electrochemical measurements, slow strain rate tension (SSRT) tests and immersion experiments. The electrochemical measurement results indicated that borate solution will facilitate the passivation film deformation on the surface of 316L stainless steel, and the corrosion resistance of 316L stainless steel decreased with the increased of pH. While the pitting corrosion of 316L stainless steel prone to occurred in the borate solution with the value of pH was 11. At the same immersion time, the number of corrosion pits increased with the pH. Furthermore, the stress corrosion cracking (SCC) susceptibility of 316L stainless steel was tested by SSRT, and suggested that higher pH leads to more sensitive, and tensile fracture morphology showed the characteristic of ductile fracture when pH was 7.

Keywords: 316L Stainless Steel, Borate Solution, pH, Stress Corrosion Cracking

1. INTRODUCTION

316L stainless steel has been widely used in nuclear power primary circuit because of its tolerance to high temperature, corrosion resistance and excellent mechanical properties [1]. In the primary circuit of pressurized water reactor (PWR), the borate solution is often used as coolant. 316L stainless steel is easy to suffer pitting corrosion and stress corrosion in this environment, which leads to the failure of PWR components and affects the safe operation of nuclear power plant. During the research we found that previous studies focused on the effect of corrosive ions (Cl⁻) on corrosion behavior of 316L stainless steel [2-5], and the effect of solution temperature on the stress corrosion behavior of 316L

stainless steel has been studied a lot [6-11], but fewer research concentrate on the pH of the solution. In the operation of PWR primary circuit, LiOH is usually added to the coolant to adjust the pH of the solution [12]. However, with the change of start-up, power operation and other conditions of the unit, the pH of the coolant will change, and 316L stainless steel is prone to corrosion under this condition [13-14].

In this paper has carried out a detailed study on the electrochemical corrosion behavior, pitting corrosion and SCC susceptibility of 316L stainless steel in borate solution with different pH. The corrosion behavior was evaluated by potentiodynamic polarization curves, electrochemical impedance spectroscopy (EIS). The effect of immersion time in different pH borate solution on pitting corrosion of 316L stainless steel was analyzed. Due to the special primary circuit conditions, the effect of different pH on SCC susceptibility of 316L stainless steel was also examined by SSRT test. The fracture characteristics of the sample were further explored by emission scanning electron microscope (SEM). The corrosion behavior of 316L stainless steel in this environment is discussed in detail, which provides a good reference for the effect of pH value on 316L stainless steel in borate solution.

2. EXPERIMENTAL

2.1 Materials

Specimens used in this work were cut from a 316L austenitic stainless steel plate, with a chemical composition is shown in Table 1.

Table 1. Chemical composition of 316L stainless steel in this study (wt.%)

Steel	C	Si	Mn	P	S	Ni	Cr	Mo
316L	0.003	0.65	1.62	0.03	0.03	12.00	17.65	2.32

The specimens were machined into two types of geometry, flat-plate electrochemical specimens and rod specimens. The electrochemical specimens with the size of $15 \times 15 \times 1.5 \text{mm}^3$. According to GB/T 15970, the shape and dimensions of rod specimen as shown in Figure 1.

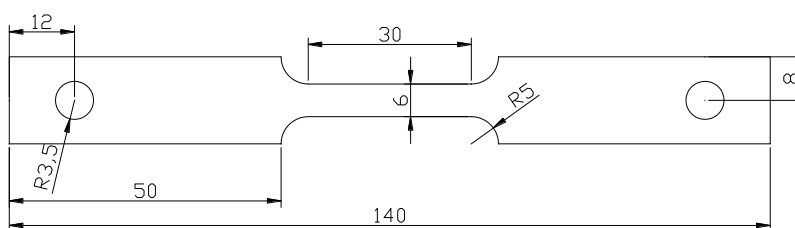


Figure 1. Slow strain rate tensile test piece size

2.2 Experimental solution

The borate solution was used to simulate the primary circuit environment of nuclear power plant. It was usually used as a coolant. All experiments were carried out in the borate solution prepared by 1100mg/L H_3BO_3 and 2.5mg/L LiOH. Adjust the pH of the solution to 7, 9, 11 with NaOH at room temperature, respectively.

2.3 Experimental equipment

Electrochemical experiment: The CHI660E electrochemical workstation made in Shanghai were conducted to the electrochemical experiments. The flat electrolytic cell was used for the electrolytic cell comprising a three-electrode system: the working electrode (316L stainless steel sheet), the reference electrode (Ag/AgCl₃ in saturated KCl), and the counter electrode (platinum sheet).

The potentiodynamic polarization curves record the current with change in potential from -0.25 V to 1.6 V, and the scanning rate is $1 \text{ mV} \cdot \text{s}^{-1}$. In the electrochemical impedance spectroscopy (EIS) tests, the frequency range from 100 kHz to 10 mHz, a wavelength of 10 mV amplitude was applied, and the data obtained from the experiment were fitted by ZSimpWin software.

The slow strain rate tensile testing instrument is a stress corrosion testing machine produced by Xi'an Lichuang Material Testing Technology Co., Ltd, and the slow strain tensile rate was selected to be $3.0 \times 10^{-6} \text{ s}^{-1}$ [15-17]. The fracture surface morphology studied by SEM of RILI SU8010.

3. RESULTS & DISCUSSION

3.1 Potentiodynamic polarization curves

Potentiodynamic polarization curves of 316L stainless steel in the borate solution with different pH were shown in Figure 2. From the potentiodynamic polarization results, the corrosion potential (E_{corr}), the passive potential range, the corrosion current density (I_p) were displayed in Table 2. It can be clearly observed that there has passivation zone in three conditions, indicating that a stable passivation film deformation on the surface of 316L stainless steel in borate solution. When the pH of the solution is 7, the range of passivation is wider than that of other conditions, which is from -0.615 to 1.043 V. Indicates that the electrochemical reaction of 316L stainless steel in neutral borate solution is hard to proceed due to the integrity and stability of the passivation film. With the increases of pH, the self-corrosion potential decrease to -0.420 V at the pH 11, and the passivation potential interval also constantly narrower which displays that corrosion of sample under borate solution with higher pH is more sensitive.

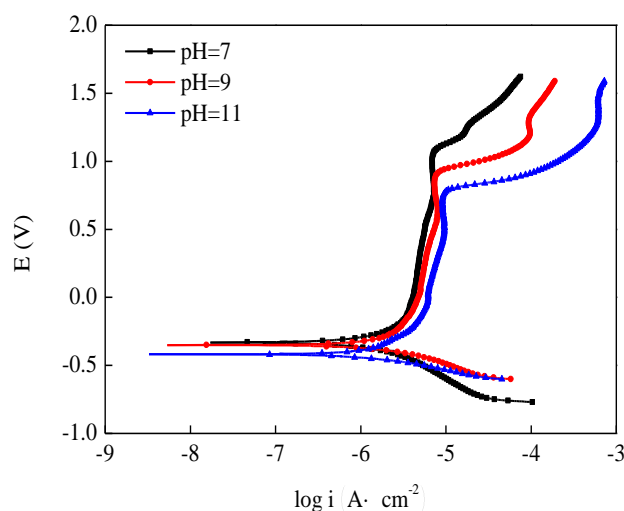


Figure 2. Polarization curve of 316L stainless steel in borate solutions with different pH

The variation of current density with corrosion potential of 316L stainless steel in the borate solution with different pH was analyzed. For all conditions, the current density of 316L stainless steel in borate solution approximately linearly increased with the increased of corrosion potential under the passivation potential interval. With the further increment of corrosion potential, current density rapid transition to exponential increase, indicating that the passivation film resistance and stability of 316L stainless steel sample is deteriorated at the pH 11. Under the influence of the electrical field, the higher current density leads to passivation film on the surface of 316L stainless steel was destroyed and the rapid dissolution of anodic, which makes the corrosion more prone to occur. It can also be observed that both in the solution of pH 9 and 11, secondary passivation occurs. Previous research points out [18] the secondary passivation of 316L stainless steel is mainly due to the convert of the composition of passivation film from low valence Cr_3O_2 and FeO to high valence Cr_2O_3 and $\text{Fe}(\text{OH})_2$ with the increase of pH, and results in the aggregation of aggressive anions on the passivation film, which may be another reason for the acceleration of corrosion caused by high pH.

Table 2. Polarization curve fitting results of 316L stainless steel in borate solutions with different pH and scan rate of $1.0 \text{ mV} \cdot \text{s}^{-1}$

pH	E_{corr}/V	Passive potential range/V	$I_p/\mu\text{A} \cdot \text{cm}^{-2}$
7	-0.328	-0.165~1.043	0.578
9	-0.350	-0.10 ~0.520	0.750
11	-0.420	-0.026~0.507	0.882

3.2 AC impedance spectrum

The results of EIS measurements of 316L stainless steel in different pH borate solution were

illustrated as Nyquist and Bode plots in Figure 3. Equivalent electrical circuit best matching the EIS spectra is shown in Figure 4.

We can see from Nyquist plots, there are two capacitance arcs which corresponding to high frequency and low frequency regions in all conditions, respectively. Indicating that the electrochemical process is completely controlled by charge-transfer [19]. The radius of the capacitance arcs represents the charge-transfer resistance. 316L stainless steel exhibited better corrosion resistance in borate solution at pH 7, it showed bigger radius in Nyquist curves. The radius of capacitance arcs decreases with the increases of pH, implying that the charge-transfer resistance deteriorated and the samples of 316L stainless steel is more prone to corrosion. Besides, high frequency region related to the resistance of the solution, which characteristic identical to Nyquist plots, the lower frequency related to polarization resistance, but the characteristic has some different [20].

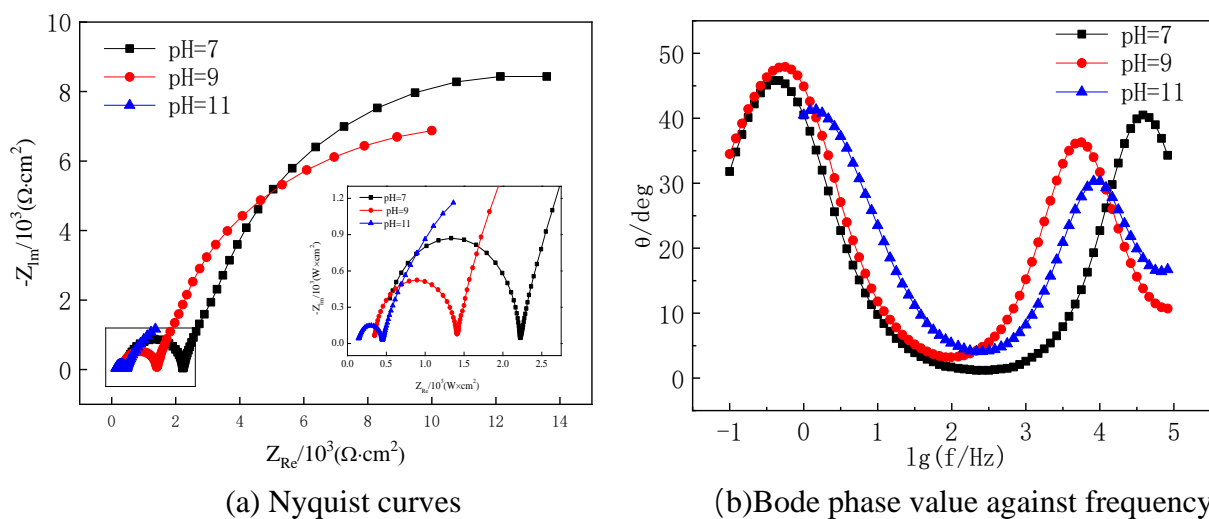


Figure 3. EIS of 316L stainless steel in borate solution with different pH (a) Nyquist curves, (b) bode phase value against frequency

An electrical equivalent circuit was used fit the EIS data, and the fitted results was listed in Table 3. Different components in the electrical equivalent circuit corresponding to different meaning [21-23]. Where R_s represents the resistance of the solution between 316L stainless steel and the reference electrode, C_1 denotes the capacitance of the passive film including the defects, R_1 is the charge transfer resistance, C_2 correspond to the subsequent passive layer, and R_2 is the resistance of passive film. It can be seen from fitting results that pH 7 has the largest value of R_1 and R_2 , and the lower value of C_1 , indicates that the electrochemical reaction is hard to carried out, the passivation film is stable and the integrity is better. With the increment of pH the corrosion resistance of 316L stainless steel was weaker than pH 7. The defects concentration of passivation film increased by several orders of magnitude results in corrosion reaction was prone to carried out. Consequently, higher pH environment has serious damage to the corrosion resistance of 316L stainless steel.

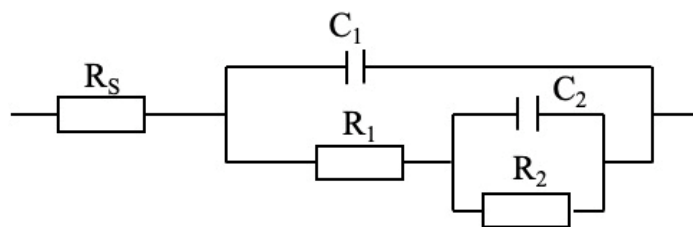


Figure 4. EIS equivalent circuit model of 316L stainless steel in borate solution with different pH

Table 3. EIS equivalent circuit fitting results of 316L stainless steel in borate solution with different pH

pH	R_s / Ω	C_1 / F	R_1 / Ω	C_2 / F	R_2 / Ω	$R_1 + R_2 / \Omega$
7	4.831	5.192×10^{-9}	1823	4.844×10^{-5}	1.447×10^5	1.465×10^5
9	355.2	5.549×10^{-8}	1123	6.016×10^{-5}	1.109×10^4	1.2213×10^4
11	145.6	9.933×10^{-6}	321.3	7.013×10^{-5}	1.802×10^3	2.1233×10^3

3.3 Pitting corrosion

In order to obtain the pitting corrosion behavior of 316L stainless steel in borate solution, the immersion experiment of 316L stainless steel was carried out. Figure 6 shows the corrosion rate of the samples under different pH solution after 30 days. The corrosion rate of 316L stainless steel in borate solution were 1.108×10^{-4} , 3.048×10^{-4} , and 8.147×10^{-4} mm/year at pH 7, 9, 11, respectively. It can be seen that the uniform corrosion rate of 316L stainless steel in the borate solution with different pH is slower, and the corrosion rate increases with the pH increase of borate solution. It is generally believed that the material can be used as nuclear power material [24] when the corrosion rate is less than 0.10 mm/a, and the experimental results meet the requirements of practical application.

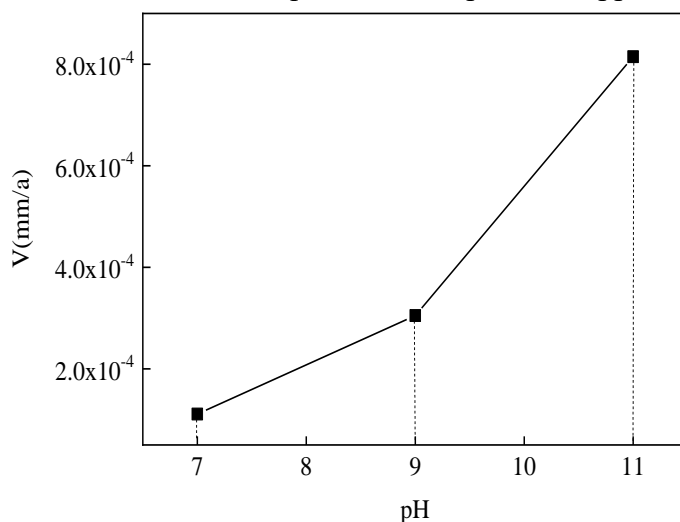


Figure 5. Immersion rate of 316L stainless steel in borate solution with different pH

As shown in Figure 6, the SEM appearance of 316L stainless steel surface after 30 days exposure time in borate solution with different pH. From the figure that when the pH value of the solution is 7, there are local corrosion pits on the surface of the sample, and occasionally small granular corrosion products can be seen. When pH was 9, the pitting pits were clearly visible under 500 times SEM, and there were corrosion products floating on the surface of the sample. It is noticeable that the corrosion intensifies and serious pitting corrosion occurs at pH 11. At this time, the number of pitting pits increases sharply, corrosion products appear in the pits, the depth of pits becomes larger, and the surface corrosion products increase. According to the electrochemical corrosion experiment results, a stable passivation film can be formed under the three conditions. When the solution at pH 7, the integrity of passivation film on the surface of 316L stainless steel is better. With the increase of pH value of solution, the surface composition of passivation film changes, and the stability becomes worse. Therefore, the occurrence of pitting corrosion may be related to the instability of the surface passivation film. When the local passivation film is destroyed by the corrosive ions BO_3^{3-} and OH^- in the solution, the pitting corrosion source will be formed. Furthermore the pitting corrosion source will gradually evolve into a corrosion hole, in which the corrosive ions were gathered and in the active dissolution state transform into anode, while the surface of 316L stainless steel which has not been destroyed transform into cathode. A micro-cell is then formed, making the localized corrosion that has been destroyed more severe [25].

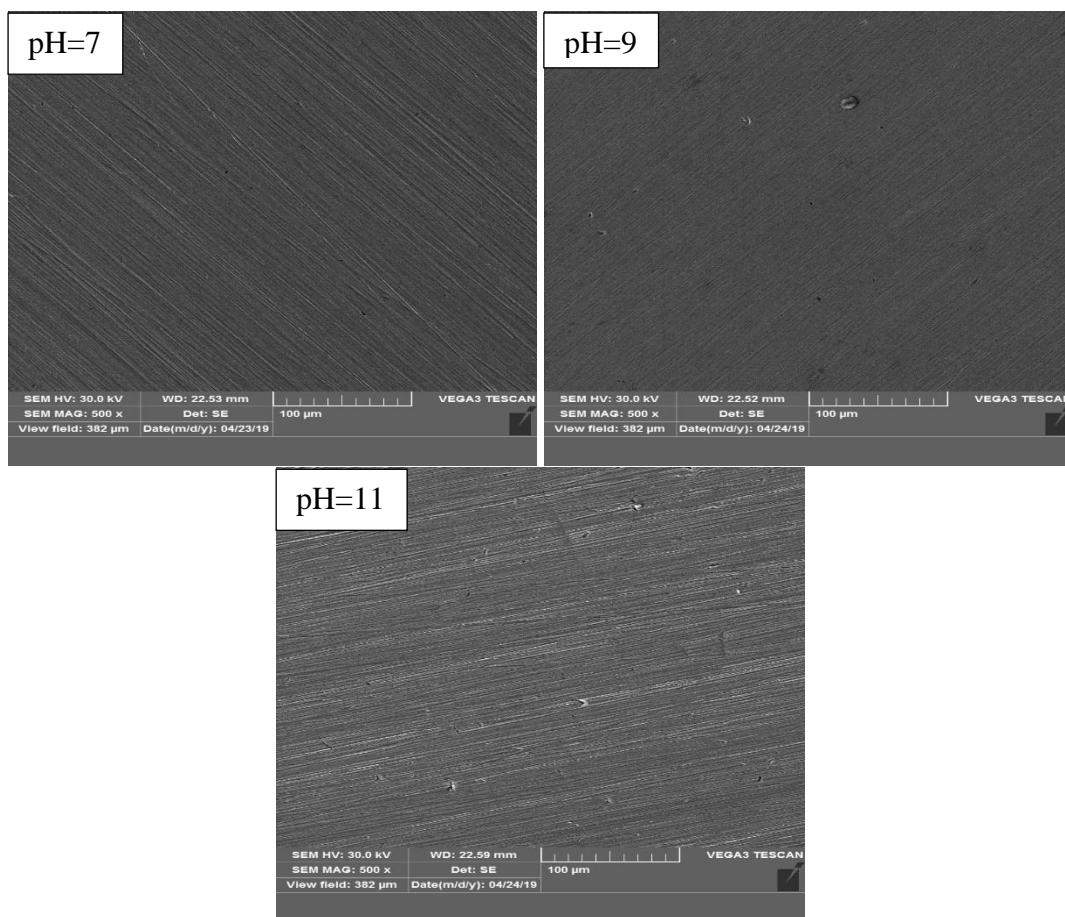


Figure 6. SEM corrosion morphology of 316L stainless steel after immersion test in borate solutions with different pH by 30 days

EDS element diagram of corrosion product at pH 11 was shown in Figure 7, in which it can be observed that the product contains of Fe, Cr and Ni et. al elements. When the pH of the solution is 11, the metallic elements in the matrix were released into the solution, and the corrosive ions in the solution diffused into the matrix, which leads to an increase in the corrosion rate of 316L stainless steel. From this, it can be seen that the main anodic reactions in the etching hole are as follows:

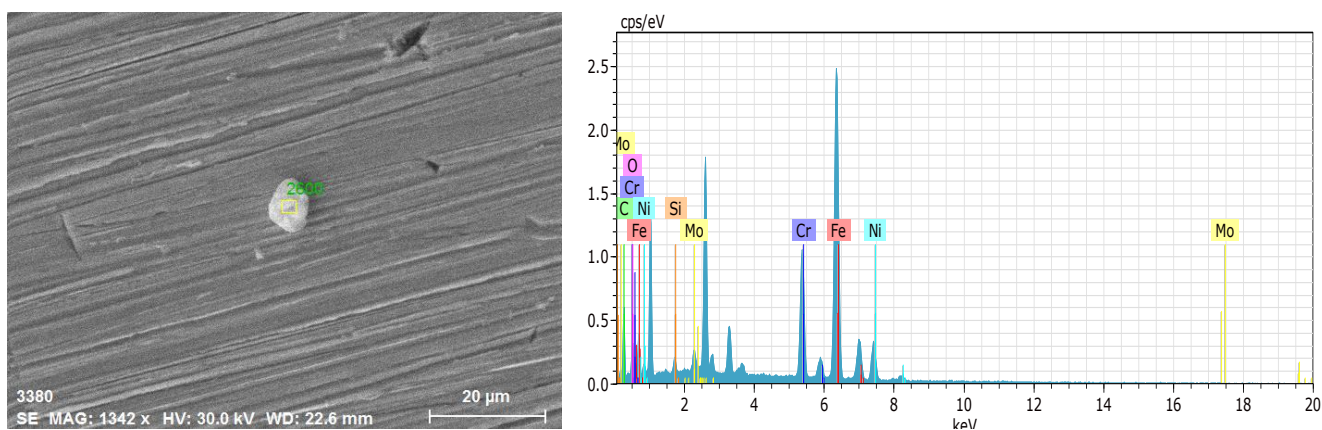
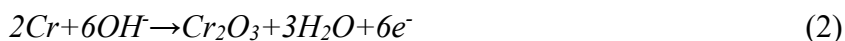


Figure 7. EDS spectrum of corrosion product after immersion for 30 days in borate solution with pH is 11

Table 4. Corrosion product element composition of 316L stainless steel in borate solution

Element	Fe	C	Cr	Ni	O	Mo	Si
Norm (wt%)	45.12	25.81	11.58	7.57	6.50	2.85	0.57
Atom (at%)	21.46	57.08	5.92	3.42	10.79	0.79	0.54

3.4 Stress corrosion behavior

The stress-strain curves of 316L stainless steel in air and borate solution with different pH was shown in figure 8. From the stress-strain results, we can see that the elongation and tensile strength of 316L stainless steel in the borate solution are lower than those in air, indicating that 316L stainless steel has a certain stress corrosion cracking (SCC) susceptibility in the borate solution. As the pH value of the borate solution increases, the elongation and tensile strength of 316L stainless steel decrease. Combination with Figure 9, the breaking time at pH 7 was longest to 70.72 h and decreases as the increment of pH. Therefore, the SCC sensitivity of 316L stainless steel increases with the increment of pH value of borate solution.

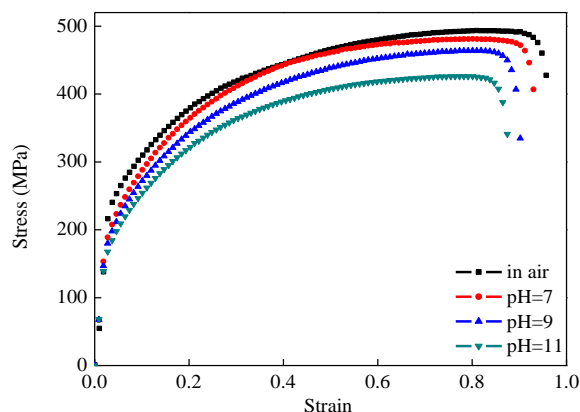


Figure 8. SSRT test results of 316L stainless steel in air and the borate solution with different pH

Previous research has indicated that the pH of borate solution is adjusted by NaOH [26-28]. With the increase of the pH value of the borate solution, the corrosive ions in the solution increase. The passive film on the surface of 316L stainless steel produced irreparable damage due to the synergistic of tensile stress and corrosive ions. The pitting corrosion will occur on the surface of the sample and the corrosion hole will be formed. The corrosion ions will enter the corrosion hole to further corrode the specimen, and then microcracks will be formed on the edge of the corrosion hole. Under the action of tensile stress, the cracks will gradually expand until the specimen breaks.

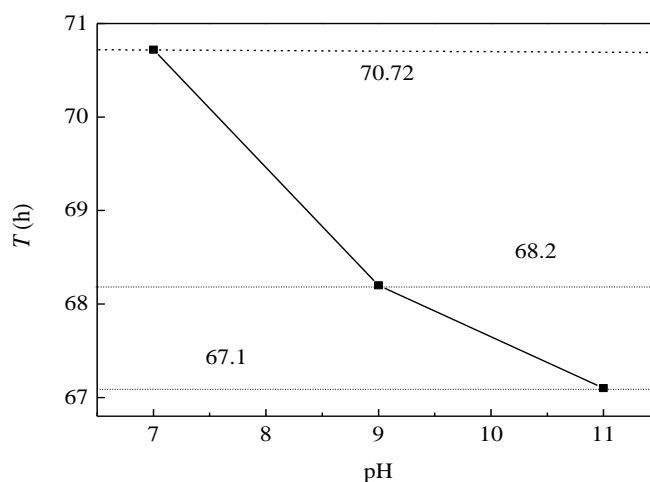


Figure 9. Fracture time of 316L stainless steel in SSRT tests in borate solution with different pH

Figure 10 presents SEM images of the fracture surface of the 316L stainless steel in the SSRT tests. Corrosion products appeared on the tensile fracture surface of 316L stainless steel in borate solution with different pH, dimples at the fracture under three conditions. It is worth noting that when the pH value of the solution is 11, a quasi-cleavage platform appears on the fracture surface, which exhibits the characteristics of brittle fracture. At this time, the fracture form of 316L stainless steel is a mixed form fracture of brittle and ductile fracture. Observe the macroscopic morphology of the fracture in three cases, the surface of the fracture is gray and shows a necking phenomenon.

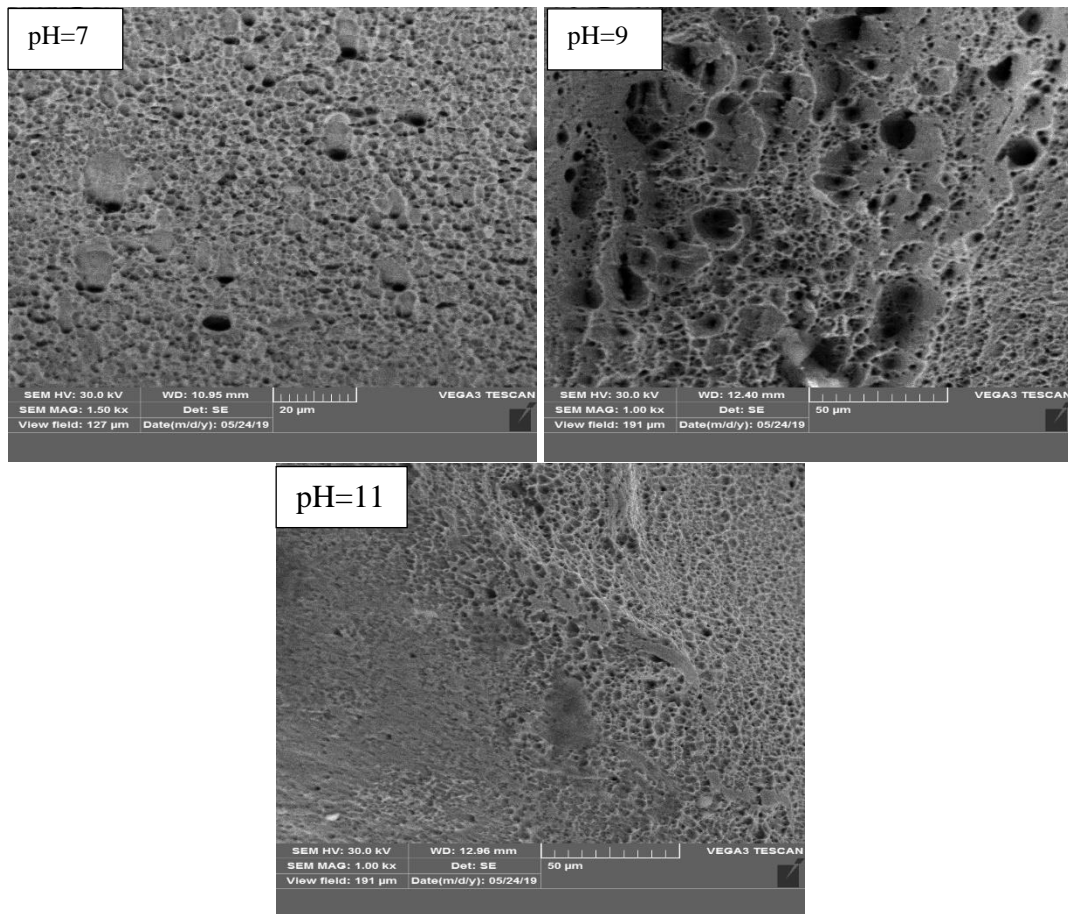


Figure 10. SEM topography of the fracture surface of 316L stainless steel in borate solution with different pH

Figure 11 is a 500 times magnified SEM view near the fracture surface of the 316L stainless steel in the SSRT tests. When the pH value is 7, the cracks near the fracture of sample are few and short. The mechanism of stress corrosion cracking can be interpreted as that the passive film on the surface of 316L stainless steel tears under the continuous tensile stress, which makes the crack tip become anode phase and propagate forward through metal dissolution, resulting in micro-cracks at the edge. With the increase of pH value of the borate solution, the microcracks near the fracture surface increased gradually. The cracks become deep and narrow when the pH of the solution is 11. At this time, the enhancement of the alkalinity of the solution makes the crack tip react fully with the solution medium, and has a higher solubility with Cr in the borate solution, which leads to the poor chromium embrittlement of the passivation film on the surface of 316L stainless steel, and the fresh metal exposed under the action of tensile stress promotes the generation and expansion of microcracks [29-30]. In combination with figure 7, the lower tensile strength of 316L stainless steel at pH 11 is related to the local poor chromium embrittlement of the sample.

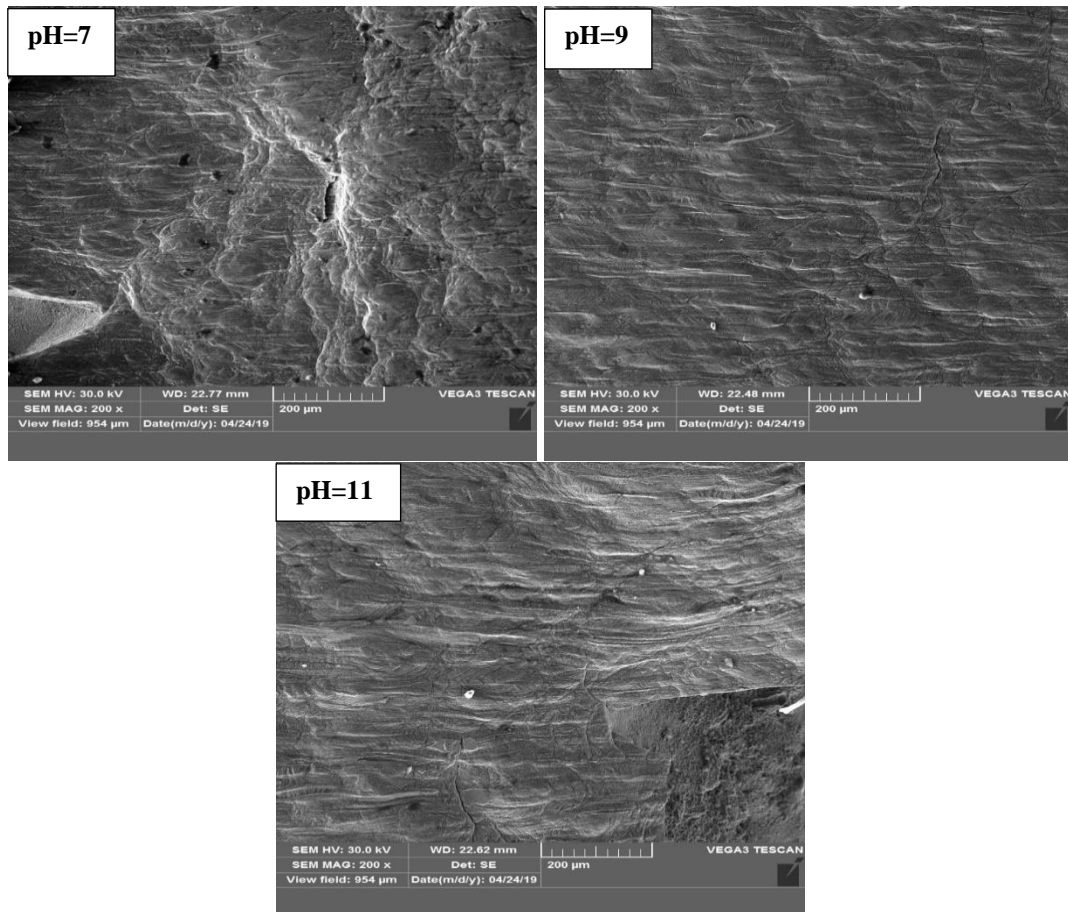


Figure 11. SEM topography of the fracture side of 316L stainless steel in borate solution with different pH

4. CONCLUSIONS

This study evaluated the effect of pH on the electrochemical and stress corrosion behavior of 316L stainless steel in the borate solution. Based on the above results and discussions, the following conclusions can be presented:

(1) Electrochemical experiments show that 316L stainless steel can form a stable passivation film in the borate solution at pH 7, 9, 11. With the increase of pH value of the solution, the composition of passivation film changes from low valence state to high valence state. The integrity of passivation film is deteriorated, resulting reduced corrosion resistance.

(2) The immersion test reveal that 316L stainless steel has good corrosion resistance, and the corrosion rate arrived to 10^{-4} grade. The occurrence of pitting corrosion is related to the integrity of the passivation film. When the local passivation film is destroyed by corrosive ions (BO^{3-} , OH^-) at high pH value, the pitting corrosion begins to germinate and grow up, accelerating the corrosion.

(3) The SSRT test displays that the SCC sensitivity of 316L stainless steel increases with the increase of solution pH value. The fracture morphology showed that the lower tensile strength was due to the local poor chromium embrittlement when the pH value of the solution was 11. At this time, the fracture corrosion cracks were deeper and the number of cracks was more.

ACKNOWLEDGEMENTS

The present research is financially supported by the National Natural Science Foundation of China (No. 51175240).

References

1. C. J. Chen, M. C. Wang, D. S. Wang, H. S. Liang and P. Feng, *Mater. Sci. Tech-lond.*, 26 (2013) 276.
2. J. Zhang, P. F. Ju, C. L. Wang, Y. C. Dun, X. H. Zhao, Y. Zuo and Y. M. Tang, *Prot. Met. Phys. Chem.*, 26 (2010) 276.
3. A. V. Bansod, N. N. Khobragade, K. V. Giradkar and A. P. Patil, *Mater. Res. Express.*, 4 (2017) 1591.
4. S. M. R. Ziaei, J. Mostowfi, M. G. Pour and S. A. R. Ziaei, *Eng. Fail. Anal.*, 33 (2013) 465.
5. M. Eskandari, M. Yeganeh and M. Motamedi, *Micro. Nano. Lett.*, 7 (2012) 380.
6. M. Matsuyama, H. Z. Shi, K. Tokunaga, A. Kuzmin and K. Hanada, *Nucl. Mater. Energy*, 16 (2018) 52.
7. S. Holdsworth, F. Scennini, M. G. Burke, G. Bertali, T. Ito, Y. Wada, H. Hosokawa, N. Ota and M. Nagase, *Corros. Sci.*, 140 (2018) 241.
8. A. Gomes, M. Navas, N. Uranga, T. Paiva, I. Figueira and T. C. Diamantino, *Sol. Energy*, 177 (2019) 408.
9. R. K. Desu, H. N. Krishnamurthy, A. Balu, A. K. Gupta and S. K. Singh, *J. Mater. Res. Technol.*, 5 (2016) 13.
10. M. Yazdkhasti, S. A. Hosseini, H. Javadinejad, H. Zare, M. S. Rizzi and H. Abedi, *Surf. Eng. Appl. Elect.*, 54 (2018) 508.
11. M. Zhu, S. Zeng, H. H. Zhang, J. Y. Li and B. Y. Cao, *Sol. Energ. Mat. Sol. C.*, 186 (2018) 200.
12. T. Yonezawa, M. Watanabe, A. Hashimoto, M. D. Olson, A. T. Dewald and M. R. Hill, *Metall. Mater. Trans. A*, 50 (2019) 2462.
13. R. L. Zhu, J. Q. Wang, L. T. Zhang, Z. M. Zhang and E. H. Han, *Corros. Sci.*, 112 (2016) 373.
14. L. T. Chang, M. G. Burke and F. Scenini, *Corros. Sci.*, 138 (2018) 54.
15. Z. Li, T. Voisin, J. T. Mckeown, J. C. Ye, T. Braun, C. Kamath, W. E. King and Y. M. Wang, *Int. J. Plasticity*, 120 (2019) 395.
16. J. G. Sezgin and J. Yamabe, *Int. J. Hydrogen Energy*, 43 (2018) 8558.
17. Y. Chen, A. S. Rao, B. Alexandreanu and K. Natesan, *Nucl. Eng. Des.*, 269 (2014) 38.
18. J. H. Ding, L. Zhang, D. P. Li, M. X. Lu, J. P. Xue and W. Zhong, *J. Mater. Sci.*, 48 (2013) 3708.
19. A. F. Alhosseini, A. Saatchi, M. A. Golozar and K. Raeissi, *J. Appl. Electrochem.*, 40 (2010) 457.
20. E. Husain, A. A. Nazeer, J. Alsarraf, K. Al-Awadi, M. Murad, A. Al-Naqi and A. Shekeban, *J. Coat. Technol. Res.*, 15 (2018) 945.
21. K. Prabakaran and S. Rajeswari, *J. Appl. Electrochem.*, 39 (2009) 887.
22. M. S. Hong, S. H. Kim, S. Y. Im and J. G. Kim, *Met. Mater. Int.*, 22 (2016) 621.
23. D. Gopi, J. Indira, L. Kavitha and J. M. F. Ferreira, *J. Appl. Electrochem.*, 43 (2013) 331.
24. M. Fregonese, H. Idrissi and H. Mazille, *J. Mater. Sci.*, 36 (2001) 557.
25. Y. H. Kim, D. G. Kim, J. H. Sung, I. S. Kim, D. E. Ko, N. H. Kang, H. U. Hong, J. H. Park and H. W. Lee, *Met. Mater. Int.*, 17 (2011) 151.
26. C. Martinez, M. Sancy, J. H. Zagal, F. M. Rabagliati, B. Tribollet, H. Torres, J. Pavez, A. Monsalve and M. A. Paez, *J. Solid State Electr.*, 13 (2019) 1327.
27. B. W. Zhang, S. J. Hao, J. S. Wu, X.G. Li, C. J. Li, X. W. Di and Y. Z. Huang, *Mater. Charact.*, 131 (2017) 168.
28. A. I. Almarshad and D. Jamal, *J. Appl. Electrochem.*, 34 (2014) 67.
29. P. Rodriguez, H. S. Khatak and J. B. Gnanamoorthy, *B. Mater. Sci.*, 17 (1994) 685.

30. R. Soulas, M. Cheynet, E. Rauch, T. Neisius, L. Legras, C. Domain and Y. Brechet, *J. Mater. Sci.*, 48 (2013) 2861.

© 2020 The Authors. Published by ESG (www.electrochemsci.org). This article is an open access article distributed under the terms and conditions of the Creative Commons Attribution license (<http://creativecommons.org/licenses/by/4.0/>).